Appl. Phys. B 65, 339–345 (1997)

Applied Physics B Lasers and Optics

Temporal characterization of ultra short laser pulses based on multiple harmonic generation on a gold surface

N.A. Papadogiannis[1,2], **S.D. Moustaizis**[1], **P.A. Loukakos**[1,2], **C. Kalpouzos**[1]

[1] Foundation for Research and Technology Hellas, Institute of Electronic Structure and Laser, P.O. Box 1527, Heraklion 71110, Greece (FAX: +30-81/391-318)
[2] Department of Physics, University of Crete, Heraklion, Greece

Received: 29 July 1996

Abstract. The simultaneous generation of second and third harmonic on a gold surface was used for the temporal characterization of an ultrashort Ti:sapphire laser pulse. In this study, a metallic surface was used in order to provide both second- and third-order interferometric (fast) and intensity (slow) autocorrelation functions for amplitude, phase, pulse profile, and temporal asymmetry measurements for ultrashort laser pulses.

PACS: 42.79.-e; 78.66.Bz; 42.65.Ky

In recent years there has been a growing interest in the development of solid-state laser systems of ultrashort pulse duration [1–3], leading to pulse durations below 100 fs, high laser peak intensities and broad frequency bandwidths. This fact gives rise to an imperative need for a precise characterization of these features of ultrashort laser pulses.

Since the late 1980s, a number of new autocorrelator techniques have been developed to achieve this goal. It would be useful to develop a compact autocorrelator which could work independently of the wavelength, bandwidth and pulse duration of the laser, and could provide both second and third order autocorrelation data using the same experimental set-up and only one nonlinear medium. Several techniques for ultrashort laser pulse characterization have been published recently [4–10] to provide pulse duration measurements, in most of the cases, or phase-sensitive information of laser pulses in others. As far as we know, there is no work in the literature that allows the simultaneous measurement of pulse duration, amplitude and phase profile of ultrashort laser pulses. Moreover, most of the existing techniques are not applicable for the extended spectral range of existing laser systems which, in most of the cases, have a very broad spectrum.

At the same time, with the development of techniques for ultrashort laser pulse characterization, several articles have appeared studying mainly the second harmonic generation from metallic surfaces [11–14], and multiphoton harmonic generation [15–17].

The above studies show that both odd and even harmonics are generated in the reflected fundamental direction when metallic surfaces are illuminated by intense laser pulses. The harmonic light is predominantly of surface origin and it depends on the component of the laser electric field that is normal to the surface: *p*-polarization-dependent. Also, the harmonics have the same polarization as the reflected fundamental, that is *p* polarized. The direction of the various harmonics is collinear to the reflected fundamental. The conversion efficiency of the second harmonic is of the order of 10^{-10} for laser intensities of the order of $1\,\mathrm{GW\,cm^{-2}}$, while the decrease of the observed intensity in the higher harmonics up to the fifth order is only a few orders of magnitude. Recent theoretical works have accounted for such experimental observations [16, 17].

Because of the continuous nature of the energy states of the conduction band of metals, the tunability of the harmonics is continuous and almost flat over a long wavelength region. This flat tunability is not observed for any short energy region in the vicinity of interband transitions. It is known that when intense (up to a few tens of $\mathrm{GW\,cm^{-2}}$) and short (a few hundreds of fs) laser pulses are incident on a metallic surface, electron relaxation phenomena affect the reflectivity [18, 19] as well as the harmonic generation [14, 20]. In contrast, when the laser pulses have an intensity of the order of a few hundreds of $\mathrm{MW\,cm^{-2}}$ subpicosecond pulse duration, nonradiative electron relaxation phenomena do not affect the harmonic generation, which is then governed purely by photodynamic laws [14].

Both odd and even harmonics generated exhibit characteristics identical to the generating laser pulse, continuous tunability and show a slow decrease in the conversion efficiency when progressing to higher orders. The above features allow for the complete characterization of ultrashort laser pulses, based on harmonic generation from metallic surfaces.

1 Experimental details

For the experimental studies, the system used was a Spectra-Physics Tsunami mode-locked Ti:sapphire laser which provided pulses of duration of about 100 fs at 800 nm and an average CW power of 0.9 W. The repetition rate of the system was 82 MHz. The system was pumped by a Spectra-Physics Beamlok Argon Ion CW laser operating at 8 W.

The nonlinear medium was a 4-μm-thick polycrystalline mirror-like gold surface. Gold was chosen because of its inertness to most substances under atmospheric conditions. The preparation of the gold surface as well as the experimental arrangement for harmonic generation, detection and data acquisition methods were similar to those used in our previous studies [13–15]. The direct output of the Ti:sapphire is guided to an autocorrelator arrangement and then focused by a thin lens on the metallic surface. The autocorrelator system is a Michelson type interferometer, in which the incident laser beam is separated in two parts by a beam splitter. One of the two laser pulses is delayed or advanced, with respect to the other, through an optical delay line of a minimum resolution of 0.1 μm. The two beams are subsequently joined collinearly and focused onto the same point of the gold surface with an angle of incidence $\theta = 72°$. A movable mirror, in conjunction with a CCD camera, can be routinely used to test the proper collinear alignment of the incident beams and to establish the zero delay. Note, that when the two beams are completely collinear and at exactly zero delay, only one very bright interference fringe exists on the CCD. The optical system does not modify the pulse duration. The above was ensured by performing similar measurements using the slightly different setup of second harmonic generation (SHG), through a BBO crystal instead of gold, as the nonlinear medium. Note, that in this alignment setup, all lenses are removed from the path of the beam.

All tests that ensure that the harmonics are produced on the gold surface as well as appear in a clear form without any considerable continuous emission background, were performed. These tests are described in detail in our previous studies [13–15]. The harmonics signal, incident on a photomultiplier, is recorded by a lock-in amplifier.

Using the above experimental setup, as shown in Fig. 1, one can obtain second and third autocorrelation curves as well as the associated spectra of the harmonics and the fundamental.

2 Results and discussion

Initially, we measured the second and third harmonic signals versus the pressure of the vacuum cell. When the pressure was varied from 10^{-8} mbar up to atmospheric pressure, no considerable change was observed in either the second or third harmonic yield. Thus, we decided to perform the experiment in air and thus simplify the experimental setup.

Varying the direction of the fundamental beam polarization at the input relative to the surface normal using a $\lambda/2$ plate, we measured the intensity of the generated second and third harmonic light. The experimental results, for laser peak intensity equal to 100 MW cm^{-2}, are shown in Fig. 2. The fitted curve is a $\cos^{2n}\phi$ function, where n is the multiphoton order and ϕ is the polarization angle. The angle $\phi = 0°$ corresponds to p polarization and $\phi = 90°$ corresponds to s polarization. This experiment proves that the effect is predominantly of surface origin and it comes from the laser-induced nonlinear current of the surface electrons [13, 15, 21, 22].

The next step, was to record the autocorrelation curves of the Ti:Sapphire laser pulses. Initially, we measured the laser pulse duration by the second-order intensity autocorrelation curve with typical results shown in Fig. 3. The peak-to-background ratio is 2.8 : 1, which is close enough to the

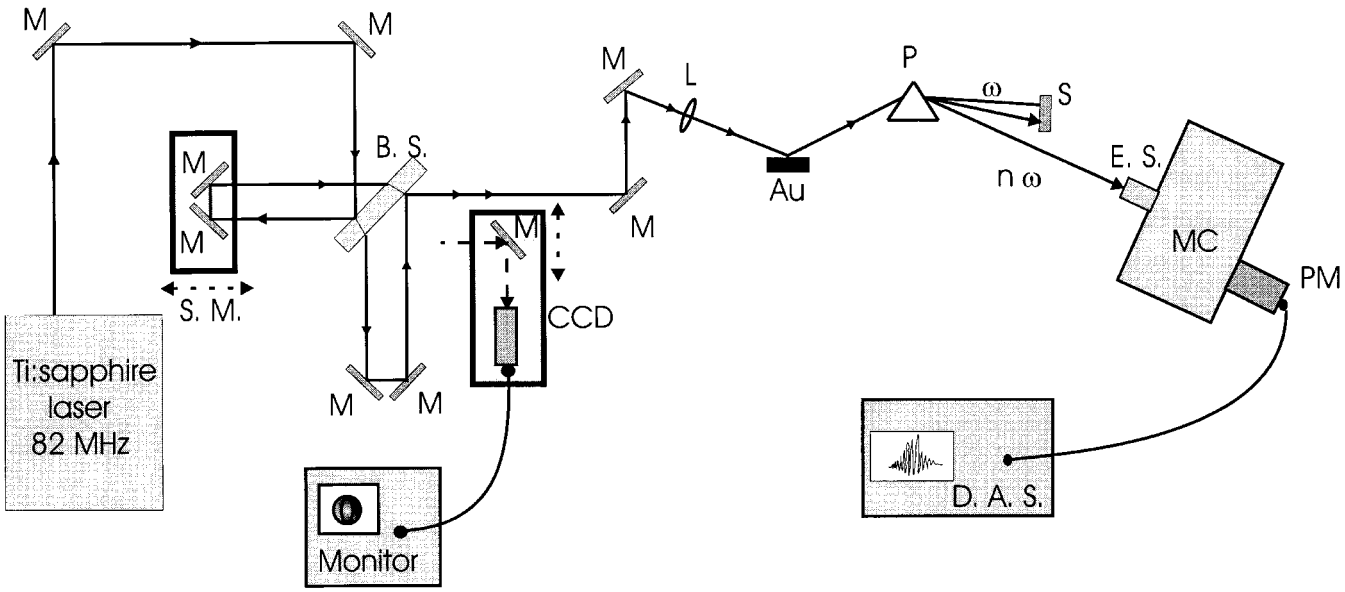

Fig. 1. Experimental setup. M: thin mirrors. L: thin lens. P: prism. S: stop. S.M.: stepper motor. B.S.: 100-μm-thick beam splitter. CCD: movable CCD camera. Au: gold surface. E.S.: entrance slit. MC: monochromator. PM: photomultiplier. D.A.S.: data acquisition system

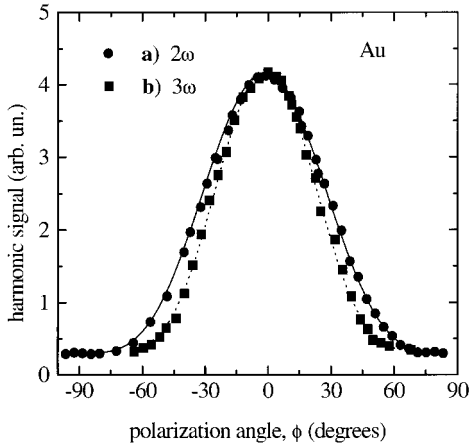

Fig. 2. a Second harmonic generation efficiency versus the polarization angle (ϕ) for an angle of incidence, $\theta = 72°$, of the Ti:sapphire laser pulses (100 fs, 800 nm), obtained from a gold surface. The solid line represents the $\cos^4\phi$ curves which show the *p*-polarization dependence of the harmonic generation as well as the second order of the phenomenon. **b** Similar to (**a**) but for the third harmonic generation. The dashed line represents the $\cos^6\phi$ function

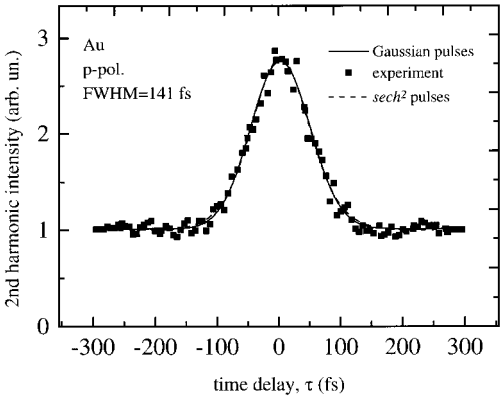

Fig. 3. Intensity second-order autocorelation curve obtained by second harmonic generation on a gold surface by Ti:sapphire laser pulses. Both Gaussian and $\mathrm{sech}^2(t)$ pulse function types fit well to the experimental data. According to the data, the FWHM of the fundamental pulses is 100 ± 2 fs for the Gaussian and 91 ± 2 fs for the sech^2 case

expected ratio, 3 : 1, for intensity second-order autocorrelation curves. The small difference is due to the fact that the two pulses of the autocorrelator were not of the same energy (energy ratio, R is 6.5 : 10).

The experimental autocorrelation curves fit well to both a Gaussian curve and the second-order intensity autocorrelation function for $\mathrm{sech}^2(t/T)$ fundamental laser pulses, that is:

$$G_{\mathrm{B}}^2 = 1 + 2r_{2\omega}\frac{(\tau/T)\coth(\tau/T) - 1}{\sinh^2(\tau/T)}\,, \qquad (1)$$

where $r_{2\omega} = (1 + R^2 + 4R)/(1 + R^2)$. The laser-pulse duration (FWHM), obtained by the autocorrelation curve, is 100 ± 2 fs for the Gaussian fitting and 91 ± 2 fs for the sech^2 case [23].

Simultaneously, we obtained the laser-pulse spectrum presented in Fig. 4. The FWHM of the Gaussian-like spectrum is 8.7 nm. The product $\Delta\nu\ \Delta t$ is obtained by the

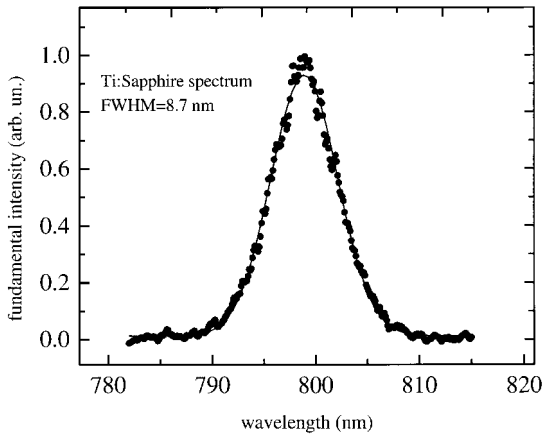

Fig. 4. Spectrum of the Ti:sapphire laser pulses used for the autocorrelation function measurements. The profile is roughly Gaussian with a 8.7 nm FWHM

experiment to be 0.41 for the Gaussian case and 0.37 for the sech^2 case. $\Delta\nu$ is the FWHM of the laser spectrum, while Δt is the obtained laser pulse duration. According to the calculation presented in [23], assuming a Gaussian laser-pulse temporal profile, the time bandwidth product should be 0.4413, while for the sech^2 case it should be 0.3148. Note, that for any other temporal profile type, the above product is much different [23]. We can infer that the Ti:sapphire laser pulses have a duration of about 100 fs with a temporal profile close to a Gaussian or a sech^2 function.

Similar results for the second-order intensity autocorrelation curves with background were observed using the second harmonic generation in a BBO crystal. The results are depicted in Fig. 5. The laser pulse profile is again Gaussian with a FWHM of 102 ± 2 fs. This confirms that the autocorrelation curves, measured via harmonic generation on gold, did not contain any relaxation phenomena that might destroy their shape and, consequently, the pulse-width measurements.

The movable branch of the autocorrelator can move with a minimum step of 0.1 μm. Since the laser wavelength is

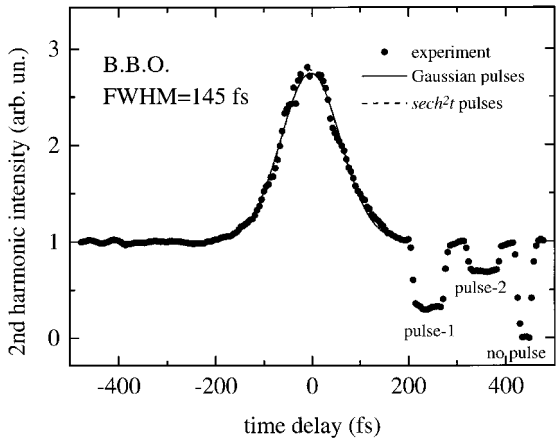

Fig. 5. Intensity second-order autocorrelation curve obtained by the second harmonic generation in a BBO crystal. The FWHM of the autocorrelation curve is 145 ± 3 fs, that is, for Gaussian laser pulse, 102 ± 2 fs and for sech^2, 94 ± 2 fs

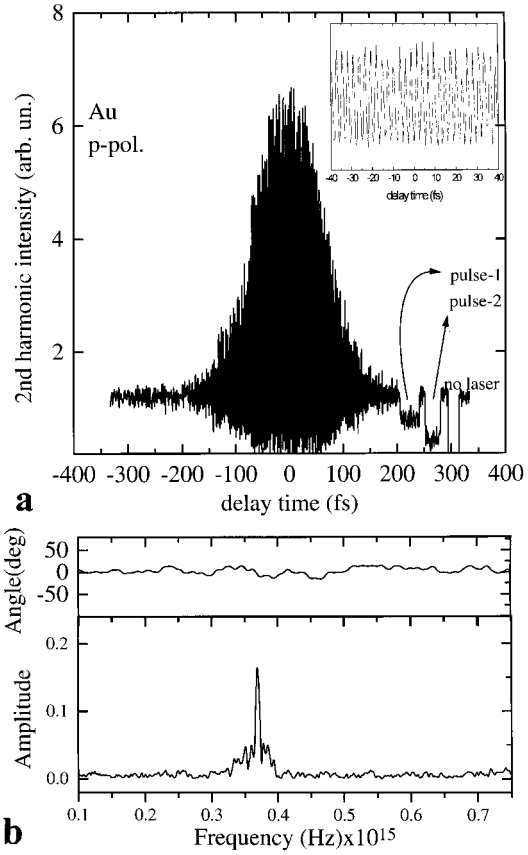

Fig. 6. **a** Interferometric second-order autocorrelation curve for 100 fs Ti:Sapphire laser pulses obtained from second harmonic generation on a gold surface. Inset: Expanded area from −40 fs to 40 fs delay time. The oscillations of electric field are observed; the period of these oscillations is 2.7 fs. **b** fast Fourier transform of the curve in (**a**). The phase has no considerable chirp and the amplitude is maximized at frequency 3.7×10^{14} Hz. This is the frequency of the 800 nm-laser pulses

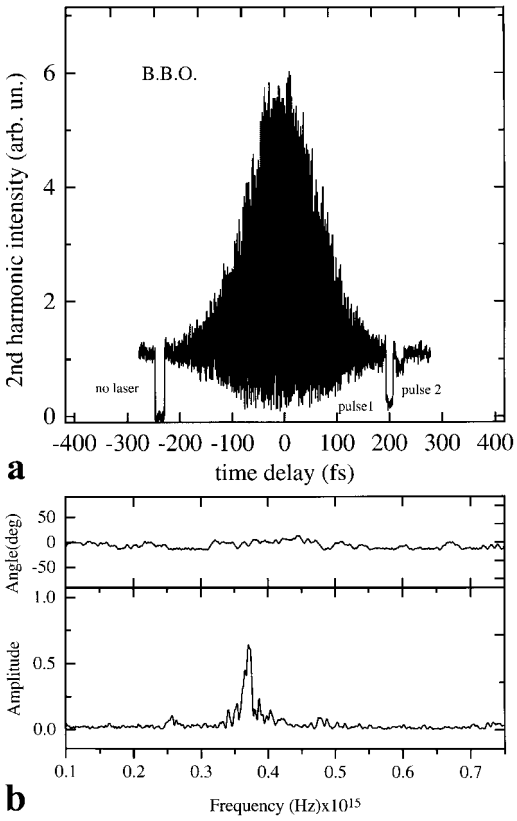

Fig. 7. Similar to Fig. 6, except that the second harmonic is obtained from a BBO crystal

0.8 μm, we were able to measure the interferometric autocorrelation curves which give additional information for the phase of the laser pulse and contain the rapid oscillations of the $\cos(\omega\tau)$ term. These curves (interferometric autocorrelation curves) are sensitive to the variations of the phase of the electric field. One of them is shown in Fig. 6a. The inset of this figure displays the period of the amplitude variations of the electric field which is 2.7 fs. This value is in excellent agreement with the period of the 800 nm wavelength laser pulse, which is 2.67 fs. Figure 6b, shows the fast Fourier transform (FFT) of the interferometric autocorrelation function. The phase of the electric field is constant, with fluctuations around zero, but the main result of the FFT is that it confirms that in the fast oscillating autocorrelation function of Fig. 6a, the basic frequency is the one of the laser pulse, 3.75×10^{14} Hz. The FWHM of the amplitude of the FFT is 4×10^{12} Hz, roughly equal to the laser-pulse bandwidth, as seen in Fig. 4.

Similar results for the interferometric autocorrelation function were obtained using the second harmonic of the laser pulse from a BBO doubling crystal. These results confirm our measurements and our analysis of the interferometric second-order autocorrelation function obtained from the gold surface. The BBO case is shown in Fig. 7.

The real electric field amplitudes can be expressed as:

$$E(t) = \xi(t)\cos[\omega t + \phi_{\mathrm{p}}(t)]\,, \tag{2}$$

where $\xi(t)$ denotes the assumed pulse shape, ω the frequency of the laser, and $\phi_{\mathrm{p}}(t)$ the phase function of the laser pulse. Assuming a Gaussian temporal profile for the function $\xi(t)$ of the electric field and a linear phase "chirp" [23], i.e., $\phi_{\mathrm{p}}(t) = at^2/T^2$, the corresponding second-order interferometric autocorrelation curves for various a are shown in Fig. 8. Here, T is the characteristic time of the Gaussian, $\mathrm{e}^{-(t/T)^2}$, temporal profile.

The resulting expression for the interferometric autocorrelation with background function, for a laser pulse described above, is [23]:

$$g_{\mathrm{B}}^2(\tau) = 1 + 4\mathrm{e}^{-(3+4a^2)\tau^2/8T^2}\cos(\omega t)\cos[a^2\tau^2/2T^2] + \mathrm{e}^{-(1+4a^2)\tau^2/2T^2}\cos(2\omega\tau) + 2\mathrm{e}^{-\tau^2/2T^2}\,. \tag{3}$$

The theoretical curve for $a = 0$ and the experimental interferometric autocorrelation curve are in satisfactory agreement. The main difference is that the experimental curve has a peak-to-background ratio of about 7 : 1 whereas for the theoretical curve it is 8 : 1. This difference is attributed to the fact that in the experiment, the two autocorrelator pulses were not identical in energy; the energy ratio is 6.5 : 10. This fact is shown clearly in the signals of the second harmonic in Fig. 6.

From the above experimental and theoretical interferometric second-order autocorrelation curves, it is clear that

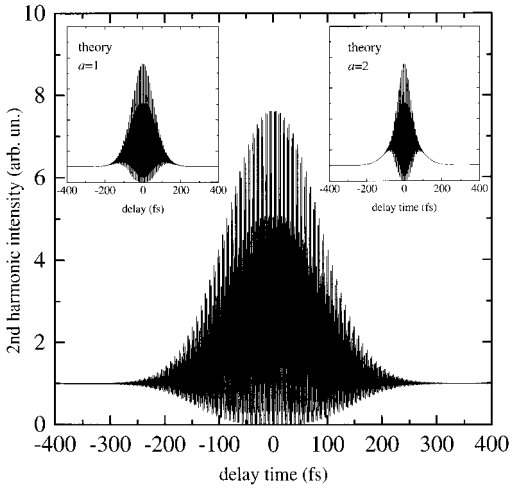

Fig. 8. Theoretical calculations for the second-order interferometric autocorrelation function assuming two identical Gaussian laser pulses with a FWHM of the slow varying envelope equal to 100 fs and a wavelength of 800 nm. The phase of the electric field is constant and equal to zero for the main figure, and it has a linear chirp with different values of the parameter a for the two small insets

the Ti:sapphire laser pulses are fully coherent, with no considerable phase chirp, having a duration of about 100 fs and a temporal profile close to Gaussian or sech^2.

Until now, there was no information for a possible pulse temporal asymmetry. The second-order autocorrelation function can not give such information for laser-pulse asymmetry since it is a fully symmetric function, even if the laser pulse has an asymmetric profile. The asymmetry of laser pulses can be deduced by third-order autocorrelation measurements [24].

Considering two laser pulses with intensity temporal profiles $I_1(t) = I(t)$, $I_2(t) = RI(t)$, where R varies between 0 and 1, the third-order intensity autocorrelation curve (TOAC) is expressed as:

$$G_{\mathrm{B}}^3(\tau) \propto (1+R^3)\langle I^3(t)\rangle + 9R\langle I^2(t)I(t+\tau)\rangle + 9R^2\langle I(t)I^2(t+t)\rangle \,, \tag{4}$$

where $\langle\rangle$ denotes time average (t), G_{B}^3 is the third-order intensity autocorelation function with background and τ is the time delay between the two laser pulses. The peak-to-background ratio, r, of the intensity third-order autocorrelation function is given by the equation:

$$r_{3\omega} = \frac{1+R^3+9R+9R^2}{1+R^3} \,. \tag{5}$$

For $R = 1$, i.e. for equal intensity laser pulses, $r = 10$.

Experimentally, the measurement of the TOAC requires a medium with observable third-order phenomena where internal relaxation processes do not influence the TOAC measurements. In the past, for TOAC measurements, the three photon fluorescence was proposed [24]. Such measurements require a triangular configuration and a fluorsciny media that exhibits resonance near 3ω, where ω is the laser photon frequency [24]. Another method used in the past is the optical Kerr effect, which is described by a third-order polarization [25]. By using an optical Kerr media, one can construct an optical Kerr gate, i.e., a Kerr cell in which the birefringence is induced by intense pump pulses.

Both techniques for TOAC measurements are limited by internal relaxation phenomena so that these methods cannot be applied to ultrashort laser pulses of the order of 100 fs or less. On the other hand, we have already shown [14] that the harmonic generation on metals, for laser intensities lower than $10\,\mathrm{GW\,cm^{-2}}$ in the femtosecond regime, is free from relaxation phenomena which take place on metallic surfaces. This fact gives an advantage for the use of surface harmonic generation for ultrashort pulse measurements and especially for TOAC measurements, where the doubling crystal technique is not applicable.

Using the same experimental configuration as for the second harmonic case, we measured the third-order intensity autocorelation curve from the gold surface. Typical results are shown in Fig. 9. This curve shows clearly that the laser pulse was, to a good approximation, symmetric. Assuming a fundamental laser pulse of the form

$$I(t) \propto \frac{1}{(\mathrm{e}^{-t/T_1} + \mathrm{e}^{+t/T_2})^2} \,, \tag{6}$$

the asymmetry of the laser pulse is described by the ratio T_2/T_1. In the case where $T_1 = T_2 = T$, the pulse is the $\mathrm{sech}^2(t/T)$, which is fully symmetric. The ratio T_2/T_1 is $1.00 \pm 0.05 (T = 42\,\mathrm{fs})$, which shows that the Ti:sapphire laser pulse was symmetric to a very good approximation. Recall that the intensity third-order autocorrelation curve can be expressed as:

$$I_{3\omega}(\tau) = (1+R^3) + 9R[G_0^3(\tau) + RG_0^3(-\tau)] \,, \tag{7}$$

where

$$G_0^3(\pm\tau) = \frac{\langle I^2(t)I(t\pm\tau)\rangle}{\langle I(t)\rangle^3} \,. \tag{8}$$

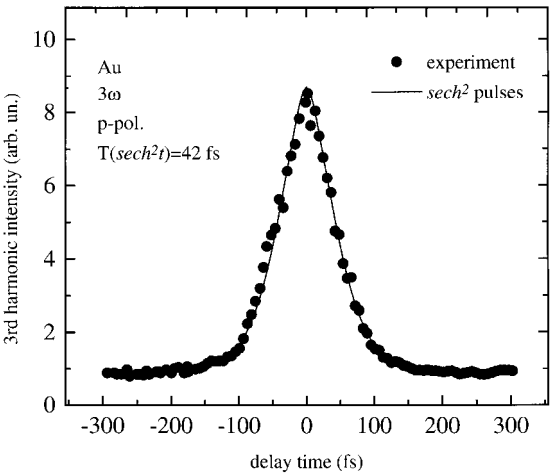

Fig. 9. Third-order intensity autocorrelation curve measured by the third harmonic generation on gold surface (*dots*). The continuous line corresponds to the theoretical fitting ($T = 42$ fs i.e., $\tau_{\mathrm{p}} = 92$ fs for the sech^2 case). The laser-pulse temporal profile is symmetric

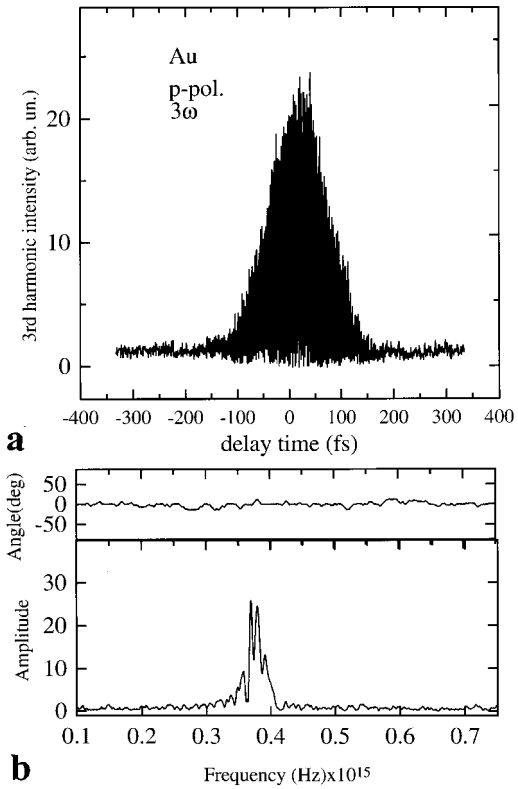

Fig. 10. Third-order interferometric autocorrelation curve obtained from the Au surface. The analysis is similar to the Fig. 6

For $I(t) = \mathrm{sech}^2(t/T)$, $G_0^3(\tau)$ is calculated to be [26]:

$$G_0^3 = \frac{15}{2\sinh^2(\tau/T)}\left[-\frac{2}{3} + \coth^2\left(\frac{\tau}{T}\right) - \frac{\tau}{T}\frac{\coth(\tau/T)}{\sinh^2(\tau/T)}\right]. \quad (9)$$

The experimental peak-to-background ratio for the TOAC depicted in Fig. 9 is $r_{3\omega} = 8.7 : 1$ as calculated from (5) when $R = 6.5 : 10$.

Using the smallest step of our stepper motor (0.1 μm), we also obtained interferometric third-order autocorrelation curves. The results are plotted in Fig. 10. In this curve, we simultaneously observe the rapid oscillations of the laser pulse electric field with a frequency of 3.7×10^{14} Hz, which is the fundamental photon frequency, as well as its temporal profile symmetry.

3 Conclusion

For the purpose of this work, the repetition rate of the laser was 82 MHz and/or 1 KHz, the energy of the laser beam was of the order of 8 nJ per pulse, practically negligible compared with the mJ or higher output energy of the state-of-the-art Ti:sapphire laser systems. The laser beam intensity on the metallic target was of the order of 100 MW cm^{-2} and the measured signal on the lockin amplifier was of the order of 2 mV. The necessary time to obtain the intensity autocorrelation curves is 10 s and about 10 min for the interferometric autocorrelation curves.

Concluding, one can say that the characterization of laser pulses using the second and third harmonic generation produced simultaneously on metallic surfaces has several advantages that make the method favorable for future use, especially for the new generation ultrashort solid-state laser systems.

These advantages are:

(a) In our previous studies, we have shown that the harmonic generation produced on metallic surfaces exhibits a flat efficiency behavior for a broad spectral range. Consequently, the autocorrelation measurements based on harmonic generation on metallic surfaces are possible over a wide spectral range. This is especially desirable for the new generation ultrashort solid-state lasers that have pulse durations as low as 10 fs and bandwidths of 100 nm, where one requires a medium with such broad tunability for nonlinear effects (harmonic generation) as can be readily supplied by metallic surfaces.

(b) The electron relaxation phenomena do not influence the harmonic generation for intensities lower than 10 GW cm^{-2}, in the femtosecond regime. Hence, the measured second- and third-order autocorrelation functions contain only the amplitude and phase variations of the fundamental laser pulse. Thus, the time resolution in such measurements is not limited by the time duration of such relaxation phenomena.

(c) Another advantage of the method is the simplicity of the experimental setup. The collinear geometry is easy to align and can easily establish the zero time delay. No special phase-matching conditions are required for the metal surface harmonic generation, that could complicate the optical geometry. In fact, the harmonic yield depends on the sum of the refractive indexes of the two frequencies rather than their difference [22]. Using exactly the same experimental setup with just one nonlinear medium (the metallic surface), one can obtain the interferometric and intensity, second- and third-order autocorrelation functions and their associated spectra.

The results presented in this study could be used to perform online time-resolved measurements by replacing the stepper motor branch of the Michelson interferometer with a continuously oscillating branch, of the order of hertz.

Acknowledgements. The authors are grateful to the European Ultraviolet Facility at FORTH-IESL supported by the Human Capital and Mobility, Access to Large Installations Plan of the European Community (ERBCHGEST 920007). We are deeply indebted to Professor C. Fotakis for his constant encouragement during this work.

References

1. D.E. Spence, P.N. Kean, W. Sibbet: Opt. Lett. **16**, 32 (1991)
2. U. Keller: Opt. Lett. **16**, 1022 (1991)
3. Ch. Spielmann, M. Lenzner, F. Krauss, R. Szipocs, K. Ferencz: Laser Focus, (December 1995)
4. K. Naganuma, K. Mogi, H. Yamada: Appl. Phys. Lett. **54**, 1201 (1989)
5. R. Trebino, C. Hayden, A.M. Johnson, W.M. Simpson, A.M. Levine: Opt. Lett. **15**, 1079 (1990)
6. A. Brun, P. Georges, G. Le Saux, F. Salin: J. Phys. D **24**, 1225 (1991)
7. R. Trebino, D.J. Kane: J. Opt. Soc. Am. A **10**, 1011 (1993)
8. D.J. Kane, A.J. Taylor, R. Trebino, K.D. Delong: Opt. Lett. **19**, 1061 (1994)
9. V. Kavelka, A.V. Masalov: Opt. Lett. **20**, 1301 (1995)
10. R.H.J. Kop, R. Sprik: Rev. Sci. Instrum. **66**, 5459 (1995)
11. K.J. Song, D. Heskett, H.-L. Dai, A. Liebsch, E.W. Plummer: Phys. Rev. Lett. **61**, 1380 (1988)

12. S. Janz, D.J. Bottomley, H.M. van Driel: Phys. Rev. Lett. **66**, 1021 (1991)
13. S.D. Moustaizis, N.A. Papadogiannis, C. Fotakis, Gy. Farkas, Cs. Toth: Appl. Phys. Lett. **67**, 3239 (1995)
14. N.A. Papadogiannis, S.D. Moustaizis, Opt. Comm. **237**, 174 (1997)
15. Gy. Farkas, Cs. Toth, S.D. Moustaizis, N.A. Papadogiannis, C.Fotakis: Phys. Rev. A **46**, R3605 (1992)
16. S. Varro, F. Ehlotzky: Phys. Rev. A **49**, 3106 (1994)
17. A.T. Georges: Phys. Rev. A **54**, 2412 (1996)
18. C.K. Sun, F. Valee, L. Acioli, E.P. Ippen, J. Fujimoto: Phys. Rev. B **50**, 15337 (1994)
19. S.D. Bronson, J.G. Fujimoto, E.P. Ippen: Phys. Rev. Lett. **59**, 1962 (1987)
20. J. Hohfeld, D. Grosenick, V. Conard, B. Matthias: Appl. Phys. A **60**, 137 (1995)
21. N. Bloembergen, R.K. Chang, S.S. Jha, C.H. Lee: Phys. Rev. **174**, 813 (1968); S.S. Jha: ibid. **145**, 500 (1966); ibid. **140**, A2020 (1965)
22. Y.R. Shen: *The Principles of Nonlinear Optics* (Wiley, New York 1984), references therein
23. K.L. Sala, G.A. Kenney-Wallace, G.E. Hall: IEEE J. Quant. Electr. QE-**16**, 990 (1980)
24. Z. Bauman: IEEE J. Quant. Electr. QE-**13**, 875 (1977)
25. L. Dahlstrom, B. Kallberg: Opt. Comm. **4**, 285 (1971)
26. J. Etchepare, G. Grillon, A. Orszag: IEEE J. Quant. Electr. QE-**19**, 775 (1983)